Stochastic dynamics for reinfection by transmitted diseases

Alessandro S. Barros*
Departamento de Física, Instituto Federal da Bahia-40110-150 Salvador, Brazil

Suani T. R. Pinho†
Instituto de Física, Universidade Federal da Bahia-40210-340 Salvador, Brazil

(Received 8 February 2016; revised manuscript received 30 April 2017; published 29 June 2017)

The use of stochastic models to study the dynamics of infectious diseases is an important tool to understand the epidemiological process. For several directly transmitted diseases, reinfection is a relevant process, which can be expressed by endogenous reactivation of the pathogen or by exogenous reinfection due to direct contact with an infected individual (with smaller reinfection rate $\sigma\beta$ than infection rate β). In this paper, we examine the stochastic susceptible, infected, recovered, infected (SIRI) model simulating the endogenous reactivation by a spontaneous reaction, while exogenous reinfection by a catalytic reaction. Analyzing the mean-field approximations of a site and pairs of sites, and Monte Carlo (MC) simulations for the particular case of exogenous reinfection, we obtained continuous phase transitions involving *endemic*, *epidemic,* and *no transmission* phases for the simple approach; the approach of pairs is better to describe the phase transition from *endemic* phase (susceptible, infected, susceptible (SIS)-like model) to *epidemic* phase (susceptible, infected, and removed or recovered (SIR)-like model) considering the comparison with MC results; the reinfection increases the peaks of outbreaks until the system reaches endemic phase. For the particular case of endogenous reactivation, the approach of pairs leads to a continuous phase transition from *endemic* phase (SIS-like model) to *no transmission* phase. Finally, there is no phase transition when both effects are taken into account. We hope the results of this study can be generalized for the susceptible, exposed, infected, and removed or recovered (SEIR_I^E) model, for which the state exposed (infected but not infectious), describing more realistically transmitted diseases such as tuberculosis. In future work, we also intend to investigate the effect of network topology on phase transitions when the SIRI model describes both transmitted diseases ($\sigma < 1$) and social contagions ($\sigma > 1$).

DOI: 10.1103/PhysRevE.95.062135

I. INTRODUCTION

Since the beginning of the last century, the mathematical modeling is a tool for studying transmitted diseases [1,2] such as childhood diseases (measles, whooping cough, chicken pox, etc.) as well as vector-borne diseases (malaria, dengue, etc.) [3,4]. More recently, due to the complex circulation of people around the world, many effects are enlarged, increasing the propagation of transmitted diseases. For instance, the cocirculation of interacting infections [5,6] is very frequent for transmitted diseases such as tuberculosis and AIDS; the reinfection effect [7] seems to become more relevant for some transmitted diseases such as tuberculosis and viral hepatitis for which patients acquire partial immunity.

For analyzing these complex situations, it would be necessary to make use of different methods. Two complementary approaches add trust to the traditional deterministic models based on population-wide random mixing, leading the models from population level to individual level: the network theory [8] and the stochastic dynamics strictly connected to percolation theory [9]. Recent results indicate that, for scenarios of cooperativity such as in interacting epidemics, hybrid first order transitions may occur on epidemic models in Erdós-Renyi networks and on d-dimensional lattices with $d \geqslant 4$ but do not occur on $d = 2$ lattices [10,11]. For some other situations, such as a model for vertically and horizontally transmitted infection, a discontinuous phase transition may occur even for $d = 2$ lattices [12].

Assuming an individual can be susceptible (S), infectious (I), and recovered (R), the SIS and SIR deterministic models are the basic models for describing the dynamics of endemic and epidemic processes, respectively. Meanwhile, the SIR model is suitable to describe the transmitted diseases with permanent immunity such as childhood diseases, and the SIS model is appropriate to describe diseases where repeated infections are common such as sexually transmitted diseases.

In the literature, some deterministic population-based models are analyzed to investigate the relevance of reinfection effect [13,14] of some transmitted diseases, such as tuberculosis, for which the individuals are temporarily protected but can be reinfected. However, the reinfection occurs with probability smaller than one. In this work, we analyze a stochastic discrete version [15,16] of a basic epidemiological model on a lattice with coordination number ζ ($\zeta = 2$ and 4), called the SIRI model (susceptible, infected, recovered, infected) [17–19], considering the probability of changing the state of a site i depending on its neighborhood. The SIR model with recurrent infection is presented in [20], wherein an infected individual may, spontaneously, become recovered, that is, acquire a permanent immunization. We intend to investigate the role of reinfection parameter, concerning the dynamical evolution to *no transmission*, *epidemic,* or *endemic* state.

Moreover, even for transmitted diseases that individuals acquire total immunity against the pathogen, due to its genetic variation, the reinfection may be associated with partial immunity against the mutant pathogen [21,22]. It has occurred,

*alessandrobarros@ifba.edu.br
†suani@ufba.br

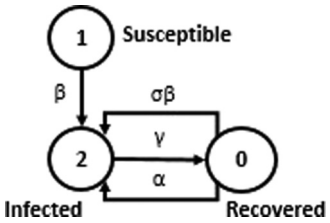

FIG. 1. Schematic representation of the SIRI model: the parameters β, $\sigma\beta$, γ, and α are, respectively, infection, exogenous reinfection, recovery, and endogenous reactivation rates.

for instance, for whooping cough outbreak that was triggered again in the United States in 2012, mainly in Washington, Iowa, and Colorado, reaching the older population [23]. Moreover, it is known that the vaccination efficiency is reduced when the recovered individual from a prime infection interacts with a mutant pathogen [24].

According to the mean-field approximations for the stochastic SIRI model, depending on the recovered rate and on the difference between the infection and reinfection rates, in this paper we obtain a continuous phase transition between *epidemic* and *endemic* regions of phase space, neglecting the endogenous reactivation. The paper is organized as follows: in Sec. II we introduce the stochastic SIRI model and its transition rate. In Secs. III and IV we present and discuss the results of the one-site and pair mean-field approximations for the particular cases of SIRI model, without endogenous reinfection (Sec. III) or without exogenous reinfection (Sec. IV). Finally, in Sec. V, we make a summary of our concluding remarks and perspectives. Among the perspectives, we call the attention to the effect of topology network on discontinuous phase transitions observed when the SIRI model describes social contagions ($\sigma > 1$) [17], mimicking a cooperative behavior analogous to coinfections in the SIR model.

II. STOCHASTIC SIRI MODEL

The SIRI model is defined on a regular lattice of N sites (see Fig. 1). A stochastic variable η_i, associated with every site i, can assume three values $\eta_i = \{0, 1, 2\}$ that correspond to susceptible, infected, and recovered states, respectively. The dynamics is asynchronous and the population is constant, that is, there is no vital dynamics. At each time, one site is randomly chosen and the following local rules are applied:

(1) A susceptible individual can become infected with a probability of infection b if at least one of its nearest neighbors is infected. The probability $(0 \to 1)$ is given by bn/ζ, where n is the number of infected neighbors and ζ is the coordination number of the network.

(2) An infected individual spontaneously recovers with probability of recovery $(2 \to 0)$ given by c.

(3) A recovered[1] individual can be reinfected in two ways:

(a) by exogenous reinfection with probability $(0 \to 2)$ given by $\sigma bn/\zeta$, if at least one of his first neighbors is infected, where σ is the reinfection coefficient;

(b) by endogenous reactivation, which occurs with probability $(0 \to 2)$ given by a.

In this work, since we are interested in analyzing the effect of reinfection for infectious diseases, whose action is smaller than prime-infection action, we consider a particular case of the stochastic SIRI model, for which the reinfection rate $\sigma\beta$ is linked to the infection rate β and it is smaller, i.e., $\sigma < 1$. Note that, in the context of social networks, it is also interesting to analyze the case $\sigma > 1$ as it was done by us and two coauthors in [17] for $\alpha = 0$.

Thus, we can understand that $\sigma < 1$ depicts the situation where the recovered individual does not acquire full immunity. Therefore, we assume σ varying in the interval $[0,1]$. Note that, for the special case where there is no reinfection ($\alpha = 0$ and $\sigma = 0$), we recover the SIR model [25,26]. Still, with $\alpha = 0$, for the limit $\sigma = 1$, the dynamic resembles the SIS model [27,28] because the recovered individual becomes susceptible to the disease with the same probability of infection ($\sigma b = b$).

Thus, there are four external parameters linked to this process: infection rate (β), endogenous reactivation rate (α), exogenous reinfection coefficient (σ), and recovery rate (γ). The rates are related to the probabilities as follows:

$$\alpha = \frac{a}{\epsilon}; \quad \beta = \frac{b}{\epsilon}; \quad \gamma = \frac{c}{\epsilon}, \tag{1}$$

with $\epsilon = \alpha + \beta + \sigma\beta + \gamma$.

Since it is a Markov process continuous time, we can conveniently rescale the time so that the rates satisfying the following condition:

$$\epsilon = 1. \tag{2}$$

Thus, α, $\sigma\beta$, β, and γ are reduced rates.

The local rules may be written through transition probability per site, in which the ith site has its state η_i is updated according to the expression

$$w_i(\eta) = \frac{\beta}{\zeta}\delta(\eta_i,1)\sum_{j\neq i}\delta(\eta_j,2) + \alpha\delta(\eta_i,0) + \frac{\sigma\beta}{\zeta}\delta(\eta_i,0)\sum_{j\neq i}\delta(\eta_j,2) + \gamma\delta(\eta_i,2), \tag{3}$$

for which the notation $\delta(r_1,r_2)$ represents the Kronecker delta.

The summations of Eq. (3) are made on the first neighbors j of the site i. The first term on the right side of Eq. (3) describes the process of infection, the following two terms represent the endogenous reactivation and exogenous reinfection, respectively, while the fourth term represents the recovery of an infected individual.

The time evolution of the probability distribution $P(\eta)$ of configuration $\eta = \{\eta_i\}$ is governed by the master equation of Markov processes:

$$\frac{d}{dt}P(\eta) = \sum_i \{w_i(A_i^-\eta)P(A_i^-\eta) - w_i(\eta)P(\eta)\}, \tag{4}$$

where A is an operator and A_i is the operator A acting on the ith site of the configuration η, that is, on the site that suffered transition, changing its state in the following order: $(1 \to 2, 2 \to 0$ and $0 \to 2)$. A^- is the inverse operator A and

[1]Note that the "recovered" individual corresponds, in this model, to an individual that may be reinfected; therefore, it may be considered a susceptible individual of type 2.

w_i corresponds to the transition probability of the site changes the site i state from η to $\eta' = A_i\eta$. The average of state function $f(\eta)$ on the distribution of probabilities $P(\eta)$ is defined by $\langle f(\eta)\rangle = \sum_\eta f(\eta)P(\eta)$.

The average of time evolution of $\langle f(\eta)\rangle$ is obtained from the master equation, written as

$$\frac{d}{dt}\langle f(\eta)\rangle = \sum_i \langle [f(A_i\eta) - f(\eta)]w_i(\eta)\rangle. \tag{5}$$

The equations of evolution for the probability $P_i(1)$ and $P_i(2)$ (the densities of susceptible and infected individuals, respectively) can be obtained from the master equation (4) using the transition probability by site of the SIRI model given by Eq. (3). Remember that $P_i(1) = \langle\delta(\eta_i,1)\rangle$ and $P_i(2) = \langle\delta(\eta_i,2)\rangle$. Thus, the time evolution equations for the first moments of the probability distribution are

$$\begin{aligned}\frac{d}{dt}P_i(1) &= -\beta P_{i,j}(12),\\ \frac{d}{dt}P_i(2) &= \beta P_{i,j}(12) - \gamma P_i(2) + \sigma\beta P_{i,j}(02)\\ &\quad +\alpha P_i(0),\end{aligned} \tag{6}$$

for which the joint probabilities $P_{i,j}(12)$ and $P_{i,j}(02)$ are given, respectively, by $P_{i,j}(12) = \langle\delta(\eta_i,1)\delta(\eta_i,2)\rangle$ and $P_{i,j}(02) = \langle\delta(\eta_i,0)\delta(\eta_i,2)\rangle$ with j as the neighboring site of i.

The equation of time evolution for $P_i(0)$, the density of recovered individuals, can be obtained from Eq. (6), due to the following normalization condition: $P_i(1) + P_i(2) + P_i(0) = 1$.

A. Mean-field approximation of one site (SMFA)

In the simplest approximation, we treat each site as if it was independent of other sites, that is, we decorrelate the joint probability as follows:

$$P_{i,j}(\eta_i\eta_j) = P(\eta_i)P(\eta_j). \tag{7}$$

Using a simplified notation $x = P_i(1)$, $y = P_i(2)$, and $z = P_i(0) = 1 - x - y$, we rewrite the system of Eq. (6):

$$\begin{aligned}\dot{x} &= -\beta xy,\\ \dot{y} &= \sigma\beta(1-x-y)y + \beta xy - \gamma y + \alpha(1-x-y).\end{aligned} \tag{8}$$

The system of differential equations (8) presents the following fixed points $E(x^*,y^*)$:

$$E_0 = (1,0); \quad E_\mp = (0,y_\mp),$$

where $y_\mp = (C \mp \sqrt{C^2 + 4\gamma\sigma\beta})/2\sigma\beta$ and $C = \sigma\beta - \alpha - \gamma$.

The first fixed point E_0 represents the *no transmission* state, where there are neither infected individuals nor recovered individuals. The second fixed point E_- has no epidemiological sense. The third fixed point E_+ represents the state for which the transmission of the disease occurs, in other words, the density of infected individuals is not null in the steady state, featuring an *endemic* state.

Performing the local stability analysis of the fixed points, the trivial fixed point E_0 is a saddle point and the fixed point E_+ is a stable node, for any positive values of rates α, β, $\sigma\beta$, and γ. Therefore, for the SIRI model with $\alpha \in (0,1)$ and $\sigma \in (0,1)$, based on the SMFA stability analysis, there is no phase transition. Thus, the absorbing state of susceptible, represented by E_0, can only be observed if the system's initial configuration is $(x_0,y_0) = (1,0)$. If the initial system configuration is $(x,y) \neq (1,0)$, the disease transmission occurs and the system evolves to a fixed point E_+.

B. Pair mean-field approximations (PMFA)

Let us assume a more realistic approximation, in which triples are uncorrelated, but we keep the correlation of the pairs. In this case, there are only three independent probabilities of pairs: $P_{i,j}(01)$, $P_{i,j}(02)$, and $P_{i,j}(12)$. Thus, the differential equations of first and second moments of the probabilities distribution are

$$\begin{aligned}\frac{d}{dt}P_i(1) &= -\beta P_{i,j}(12),\\ \frac{d}{dt}P_i(2) &= \beta P_{i,j}(12) + \sigma\beta P_{i,j}(02) + \alpha P_i(0) - \gamma P_i(2),\\ \frac{d}{dt}P_{i,j}(01) &= -\frac{(\zeta-1)}{\zeta}[\beta P_{i,j,k}(012) + \sigma\beta P_{i,j,k}(201)] + \gamma P_{i,j}(12) - \alpha P_{i,j}(01),\\ \frac{d}{dt}P_{i,j}(12) &= -\beta\frac{(\zeta-1)}{\zeta}[P_{i,j}(12) - P_{i,j,k}(112) + P_{i,j,k}(212)] + \sigma\beta\frac{(\zeta-1)}{\zeta}P_{i,j,k}(102) - \gamma P_{i,j}(12) + \alpha P_{i,j}(12),\\ \frac{d}{dt}P_{i,j}(02) &= \frac{\beta(\zeta-1)}{\zeta}P_{i,j,k}(012) - \gamma[P_{i,j}(02) - P_{i,j}(22)] + \frac{\sigma\beta(\zeta-1)}{\zeta}[P_{i,j,k}(002) - P_{i,j,k}(202)]\\ &\quad - \frac{\sigma\beta(\zeta-1)}{\zeta}P_{i,j}(02) + \alpha[P_{i,j}(00) - P_{i,j}(02)].\end{aligned}$$

The second moment's equation of the distribution is dependent on the third-order msd10oment's equations. Applying the pair mean-field approximations (PMFA) to truncate the dependence of the correlation between the probabilities of second order, the triple correlations are approximated to

$$P_{i,j,k}(\eta_i\eta_j\eta_k) = \frac{P_{i,j}(\eta_i\eta_j)P_{j,k}(\eta_j\eta_k)}{P_j(\eta_j)}. \tag{9}$$

Using a simplified notation $x = P_i(1)$, $y = P_i(2)$, $u = P_{i,j}(01)$, $v = P_{i,j}(12)$, $w = P_{i,j}(02)$ and applying PMFA, we can rewrite the previous system as follows:

$$\begin{aligned}
\dot{x} &= -\beta v,\\
\dot{y} &= \beta v + \sigma\beta w + \alpha(1-x-y) - \gamma y,\\
\dot{u} &= -\frac{\beta(\zeta-1)}{\zeta}\frac{uv}{x} + \gamma v - \frac{\sigma\beta(\zeta-1)}{\zeta}\frac{wu}{(1-x-y)} - \alpha u,\\
\dot{v} &= -\left(\frac{\beta}{\zeta} + \gamma - \alpha\right)v + \frac{\beta(\zeta-1)}{\zeta}\frac{v(x-u-2v)}{x} + \frac{\sigma\beta(\zeta-1)}{\zeta}\frac{uw}{(1-x-y)},\\
\dot{w} &= \frac{\beta(\zeta-1)}{\zeta}\frac{uv}{x} - \gamma(2w-y+v) - \frac{\sigma\beta}{\zeta}w + \frac{\sigma\beta(\zeta-1)}{\zeta}\frac{w(1-x-y-u-2w)}{(1-x-y)} + \alpha(1-x-y-u-2w),
\end{aligned} \tag{10}$$

where $x \neq 0$ and if $y = 0$, necessarily, $x \neq 1$.

Solving the system of the equations (10), we find an infinite number of fixed points:

$$E^* = (x^*, y^*, 0, 0, w^*),$$

wherein y^* and w^* are

$$y^* = \frac{(x^*-1)[\gamma\zeta - \sigma\beta(\zeta-1)]}{\sigma\beta(\zeta-1) - \gamma},$$

$$w^* = \frac{\gamma(x^*-1)[\gamma\zeta - \sigma\beta(\zeta-1)]}{\sigma\beta[\sigma\beta(\zeta-1) - \gamma]}$$

for any value of $0 < x^* < 1$.

Differently from SMFA, in site pairs there is no trivial fixed point. The system (10) does not allow the density of susceptible individuals (x) to be zero. Analyzing the fixed point E^*, the stationary density of infected (y^*) will only be positive if $\frac{\sigma\beta(\zeta-1)}{\zeta} < \gamma < \sigma\beta(\zeta-1)$. Note that if the density of susceptible individuals is equal to one ($x = 1$), it implies that $y = 0$, which is not possible [see system (10)]. Thus, to study pair approximation we have to have at least one recovered or infected individual in the initial configuration.

In order to understand the influence of the effects of exogenous reinfection and endogenous reactivation in the dynamical transmission of infectious diseases, we will study each effect separately.

III. EXOGENOUS REINFECTION

In the particular case of the SIRI model, wherein $\alpha = 0$ and $0 < \sigma < 1$, we neglect spontaneous reactivation of the pathogen, i.e., the reinfection only occurs if the individual, due to directed contact with infected neighbors, acquires a new pathogen. Note that the rate of reinfection ($\sigma\beta$) is smaller than the primary infection rate (β): so, it differs from the SIS model ($\sigma = 1$) and from the SIR model ($\sigma = 0$).

With the aim of illustrating a comparison between the SIRI model with SIS and SIR models, in terms of the reinfection effect, we simulate the SMFA and PMFA of the SIRI model for $\alpha = 0$ and different values of σ, keeping fixed the value of β. In Fig. 2(a), we show the time series of infected individuals resulting from the numerical integrations of system (8); the simulations of SMFA make evident that the reinfection effect increases the size of outbreaks in relation to the SIR model, leading from epidemic to endemic behavior until the limit case of the SIS model. This effect is also observed in Fig. 2(b) resulting from the numerical integrations of system (10) indicating that PMFA of the SIRI model leads to smaller peaks of outbreaks than its SMFA. In general, the threshold value of σ is smaller for SMFA than for PMFA; for that set

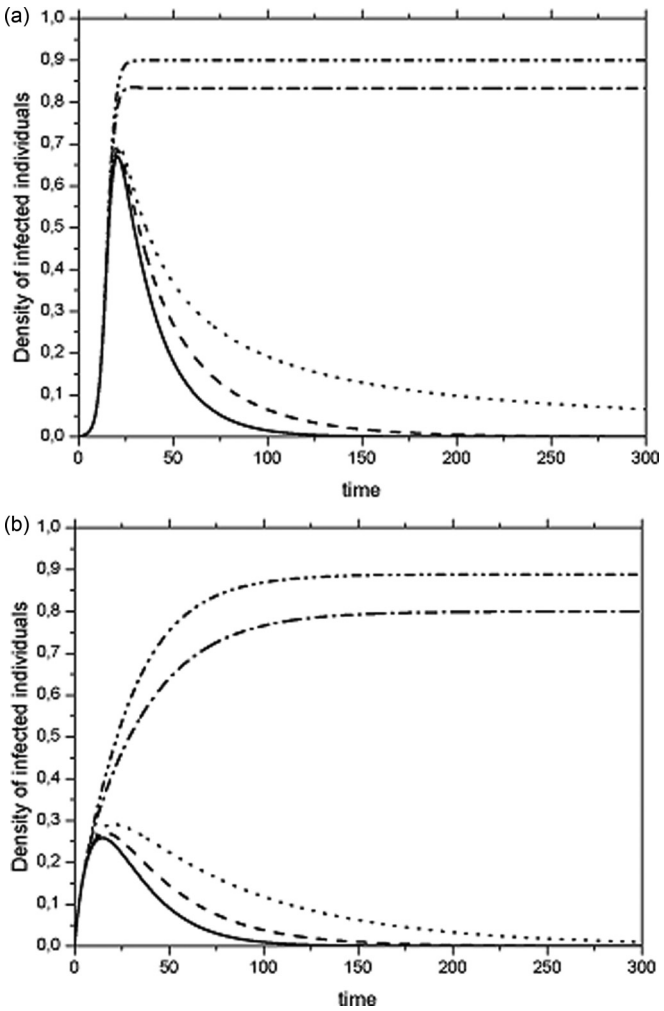

FIG. 2. Time series of infected individuals of SIRI model ($\alpha = 0$) with $\beta = 0.5$ and $\gamma = 0.05$ for mean-field approximations; $\sigma = 0$, SIR model (solid line), $\sigma = 0.05$ (dashed line), $\sigma = 0.6$ (dotted-dashed line), and $\sigma = 1$, SIS model (dotted dotted-dashed line). (a) For SMFA, the threshold value is $\sigma = 0.1$ (dotted line); (b) for PMFA: the threshold value is $\sigma = 0.1/0.85 \approx 0.118$ (dotted line).

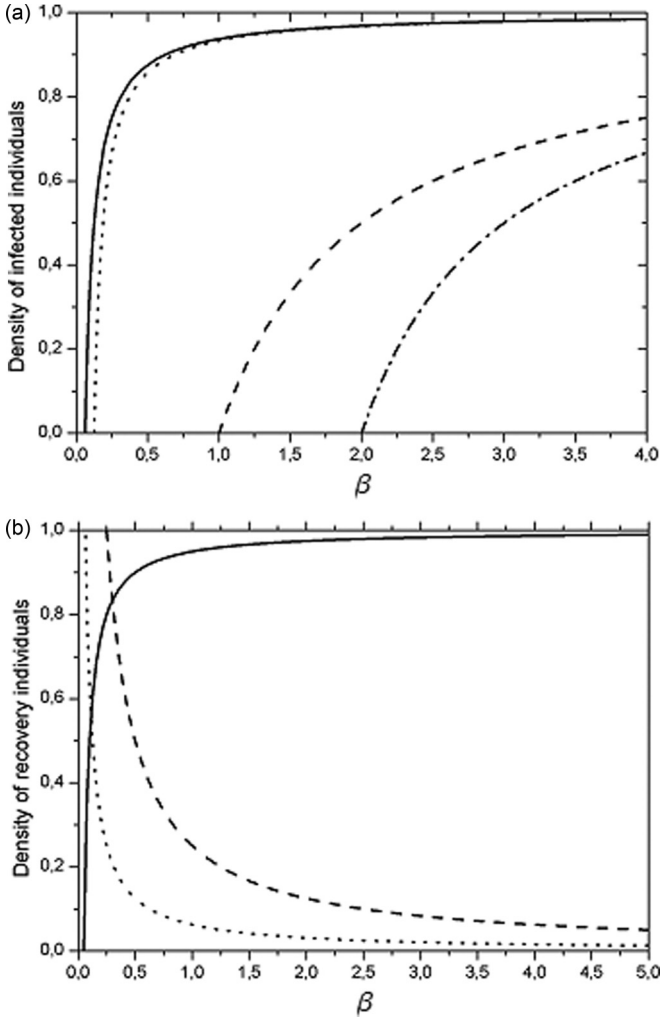

FIG. 3. Comparison between SIRI model ($\alpha = 0$) and its particular cases in terms of the primary infection rate β. Assuming $\gamma = 0.05$, (a) the density of infected individuals versus β: in case of SMFA for $\sigma = 0.8$ (solid line) and $\sigma = 1$ (dashed line) generating $\beta_{th} = 0.05$ and $\beta_{th} = 1$, respectively; in case of PMFA, for $\sigma = 0.8$ (dotted line) and $\sigma = 1$ (dotted-dashed line) generating $\beta_{th} = 0.1$ and 2, respectively; (b) in case of SMFA the density of recovered individuals versus β for $\sigma = 0.2$ (dotted line), $\sigma = 0.8$ (dashed line), and $\sigma = 0$ (solid line) (SIR model) generating $\beta_{th} = 0.04$, $\beta_{th} = 0.4$, and $\beta_{th} = 0.05$, respectively.

of parameters, the threshold value of σ is 0.1 and 0.118 for SMFA and PMFA, respectively.

Moreover, keeping fixed the reinfection effect of the SIRI model, we choose two non-null values of σ ($\sigma = 0.8$ and 0.2) for comparison of the threshold value of primary infection rate β (set up as the control parameter) as well as the intensity of endemics (for SIS and like-SIS models) for the larger value of σ and the intensity of outbreak (for SIR and like-SIR models) for the smaller value one. In the first case, looking at the density of infected individuals as the order parameter [see Fig. 3(a)], we set up that the SIRI model generates stronger endemics than the SIS model. It also presents a smaller threshold value of primary infection parameter β than for the SIS model in both cases: SMFA ($\beta_{th} = 0.05$ in contrast to $\beta_{th} = 1$ for the SIS model) and PMFA ($\beta_{th} = 0.1$ in contrast to $\beta_{th} = 2$ for the SIS model). In the second case for which the density of recovered individuals is the order parameter [see Fig. 3(b)], the SIRI model presents a smaller threshold value of primary infection parameter β than for the SIR model in SMFA ($\beta_{th} = 0.4$ in contrast to $\beta_{th} = 0.5$ for the SIR model). In pairs the density of recovered individuals only depends on the coordination number for the SIR model [26].

A. SMFA ($\alpha = 0$)

In the simple approximation, we made $\alpha = 0$ in the system of differential equations (8), and we obtain the fixed points

$$E_0^* = (x^*, 0); \quad E_1^* = \left(0, 1 - \frac{\gamma}{\sigma\beta}\right),$$

with $0 < \sigma < 1$.

The fixed point E_0^* corresponds to the infinite number of absorbing states [29], i.e, for which we can find a disease-free population. If the stationary density of infected individuals (y^*) is null, the transmission of the disease ceases (or even not happens). The point E_1 represents a population for which the density of infected and recovered individuals is non-null, i.e., the transmission of the disease persists in the population.

Based on the local stability analysis, E_0^* will be unstable if $x^* > (\gamma - \sigma\beta)/[\beta(1-\sigma)]$. At the initial phase ($t = 0$), in order to observe the disease spreading, i.e., E_1^* stable, we must have $\dot{y} > 0$ and $\dot{x} < 0$, or $x_0 > x^* > (\gamma - \sigma\beta)/[\beta(1-\sigma)]$, wherein x_0 is the initial number of susceptible individuals.

The phase diagram is constructed using only two parameters; with this aim, we made a change of variable by transforming

$$\begin{aligned} \sigma\beta &= \frac{(1-\gamma)}{2} - p, \\ \beta &= \frac{(1-\gamma)}{2} + p, \\ \gamma &= \gamma, \end{aligned} \tag{11}$$

wherein the parameter $p = \beta(1-\sigma)/2$ with $p \in [0, 1/2]$, $\sigma \in [0,1]$, and satisfying the condition (2). Performing this transformation, we can design the parameter space defined on the surface R^3 to a plane $p \times \gamma$.

The critical threshold of the epidemic for this particular case in the SMFA is

$$p_c = \frac{1 - 3\gamma}{2 - 4x^*}. \tag{12}$$

For the infinite number of fixed points that represent a disease-free population, we can highlight the following:

(1) The trivial fixed point $E_{x=1}^* = (x^*, y^*) = (1,0)$ represents the absorbing susceptible state, wherein there is no disease transmission, and it is stable if $\gamma > \beta$, i.e., the critical threshold of transition between *no transmission* and *epidemic* states is given by the line $p = (3\gamma - 1)/2$.

(2) The fixed point $E_{x=0}^* = (x^*, y^*) = (0,0)$ represents the absorbing recovered state, the extreme case where all individuals have been infected and are recovered; it is stable if $\gamma > \sigma\beta$, i.e., the critical threshold of transition between *epidemic* and *endemic* states is given by the line $p = (1 - 3\gamma)/2$.

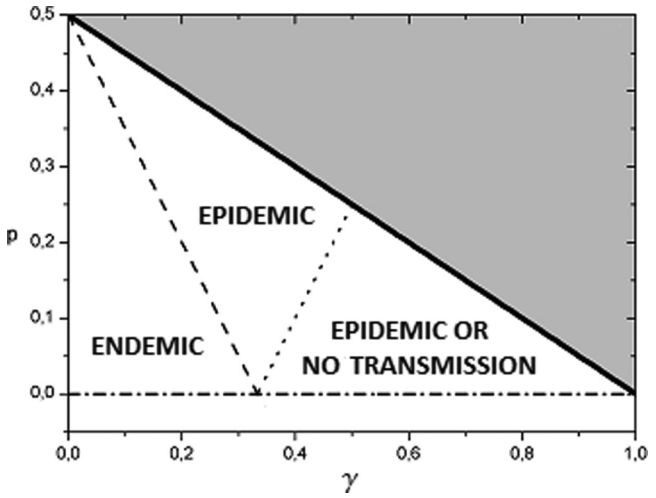

FIG. 4. Phase diagram of the SIRI model ($\alpha = 0$ and $0 < \sigma < 1$) in the SMFA, wherein $p = \beta(1-\sigma)/2$. The bold line corresponds to $\sigma = 0$; the dotted line and dashed line are such that $p_c = (1-3\gamma)/2$ and $p = (-1+3\gamma)/2$, respectively; finally, the dotted-dashed line corresponds to $\beta = 0$.

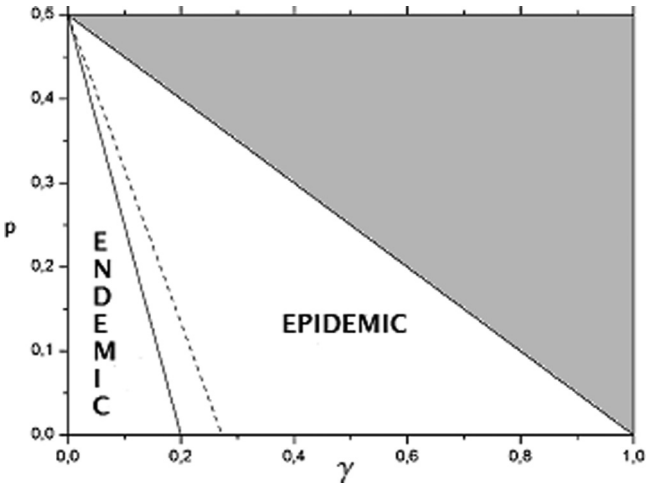

FIG. 5. Phase diagram of the SIRI model ($\alpha = 0$ and $0 < \sigma < 1$) in the PMFA for $\zeta = 2$ (solid line) and $\zeta = 4$ (dashed line), that correspond, respectively, to $p_c = (1-5\gamma)/2$ and $p_c = (3-11\gamma)/6$.

(3) The fixed point E_1^* represents the state in which the transmission of the disease persists in the population; it is stable if $\sigma\beta > \gamma$, the critical threshold of transition between *endemic* and *epidemic* states is given by the line $p = (1-3\gamma)/2$.

Thus, for SMFA, the phase diagram, shown in Fig. 4, exhibits a continuous phase transition. Thus, when the reinfection rate is larger than the recovery rate, $\sigma\beta > \gamma$, the system evolves to the *endemic* state. The line $p_c = (3\gamma - 1)/2$ defines the region of costability, wherein the system may present transmission (*epidemic phase*) or *no transmission*.

The *endemic* region represents a population where the disease activity persists and the density of infected individuals is non-null in the stationary state. In the *epidemic* region, there are no infected individuals at steady state, but there is recovered individuals due to the transmission of the disease. In the *no transmission* region, there is no activity of the disease at any time.

B. PMFA ($\alpha = 0$)

For the two-site approximation, assuming $\alpha = 0$ in the system of differential equations (10), we obtain the fixed points $E_i = (x^*, y^*, u^*, v^*, w^*)$:

$$E_0 = (x^*,0,0,0,0),$$
$$E_1 = (x^*,0,u^*,0,0),$$
$$E_2 = \left(x^*,(x^*-1)B,0,0,-\frac{\gamma(x^*-1)}{\beta\sigma}B\right),$$

wherein $0 < x^* < 1$ and $B = [\gamma\zeta - \beta(\zeta-1)\sigma]/[-\gamma + \beta(\zeta-1)\sigma]$.

The fixed point E_0 is marginally stable if $\sigma < \gamma\zeta/(\gamma - 1 + \zeta - 2\gamma\zeta)$. Applying the same change of variables made in the SMFA, we can set up the phase diagram in terms of the variables p and γ. So, there is a phase transition for which the critical threshold is given by

$$p_c = \frac{\gamma - 1 + (1-3\gamma)\zeta}{2\zeta - 1}, \tag{13}$$

such that, above this threshold value, the reinfection is active. The transition occurs at $p_c = (1-5\gamma)/2$ for a chain ($\zeta = 2$) and at $p_c = (3-11\gamma)/6$ for a lattice with coordination number $\zeta = 4$.

In Fig. 5, we represent the phase diagram for PMFA, showing the continuous phase transition between the *endemic* and *epidemic* regions. Differently from SMFA, we do not observe costability using pair approximation. We note that there is disease activity in all regions, without *no transmission* region. For PMFA, the *endemic* region is larger for $\zeta = 4$ than for $\zeta = 2$, while for SMFA the *endemic* region does not vary with coordination number of the lattice as it was expected.

Comparing the phase diagrams for SMFA (Fig. 4) and for PMFA (Fig. 5), it is easy to see that, for some parameter values, the reinfection effect for SMFA is able to keep an endemic state, but not for PMFA as it is illustrated in Fig. 6 where the value of reinfection parameter σ is fixed. It indicates that the threshold value of reinfection parameter is higher for PMFA than for SMFA.

In order to keep working with control parameter p, we set up the threshold value of p for both approximations and for Monte Carlo simulations. In Fig. 7(a), we construct the graphic $y \times p$ to show the relationship between the number of infected individuals and the parameter p. This graphic is obtained by stationary density of infected individuals y^* for a lattice in the SMFA and PMFA. Fixing $\gamma = 0.05(\text{t.u.})^{-1}$ using a generic time unit (t.u.), the critical values obtained for the approximations are $p_c^S = 0.425$ and $p_c^P = 0.374$ in the SMFA and PMFA, respectively.

Performing Monte Carlo simulations of the SIRI model on chains [see Fig. 7(b)], we conclude that PMFA leads to a better description of the model than SMFA since the threshold value of p, obtained by the second order cumulant analysis, is $p_c = 0.309$.

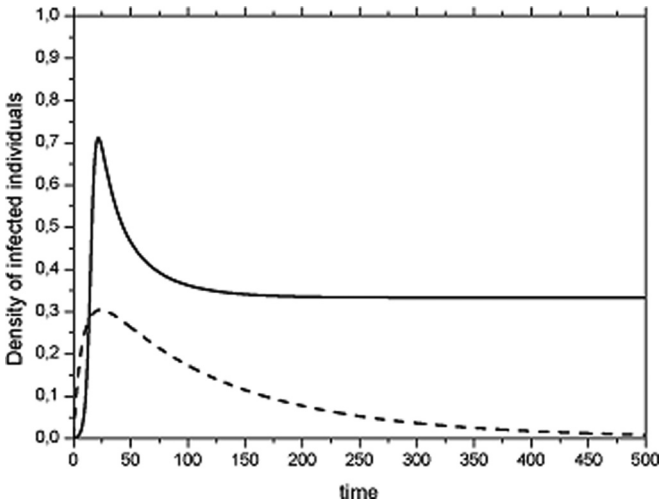

FIG. 6. Time series of infected individuals of the SIRI model ($\alpha = 0$) assuming $\beta = 0.5$; $\gamma = 0.05$ and $\sigma = 0.11$ for SMFA (solid line) and PMFA (dotted line).

IV. ENDOGENOUS REACTIVATION

In this particular case, wherein $0 < \alpha < 1$ and $\sigma = 0$, we are disregarding the effect of exogenous reinfection. This means that the individual will not be reinfected if placed in contact with infected individuals, but there is a chance that the pathogen acquired in the primary infection reactivates spontaneously. We study this effect for the SIRI model behavior, making the endogenous reactivation rate α to vary in the range [0,1].

A. SMFA ($\sigma = 0$)

Assuming $\sigma = 0$ in the system of differential equations (8), we obtain the fixed points $E = (x^*, y^*)$:

$$E_0 = (1,0); \quad E_2 = \left(0, \frac{1}{1+\frac{\gamma}{\alpha}}\right).$$

The trivial fixed point E_0 represents the absorbing state of susceptible individuals, meanwhile, the fixed point E_2 corresponds to a state which there is disease transmission. Similar to the general model (with endogenous reactivation and exogenous reinfection), this particular case does not present absorbing states of susceptible and recovered individuals. Therefore, if there is, at least, an individual porting the disease's pathogen, the transmission persists in the stationary regime.

We note that, for the stationary state E_2, $\alpha = \gamma$ corresponds to the state that the density of infected (y^*) and recovered (z^*) individuals are equal to 0.5; in other words, half of the population will have the pathogen of the disease in the steady state. For $\alpha \gg \gamma$, the density of infected individuals tends to one ($y^* \to 1$) and the density of recovered individuals tends to zero ($z^* \to 0$); for $\alpha \ll \gamma$, the density of infected individuals tends to zero ($y^* \to 0$) and the density of recovered individuals tends to one ($z^* \to 1$).

Assuming positive values for rates α, β, and γ, the trivial fixed point E_0 is always a saddle point; the point E_2, corresponding to the state of disease activity, is asymptotically stable.

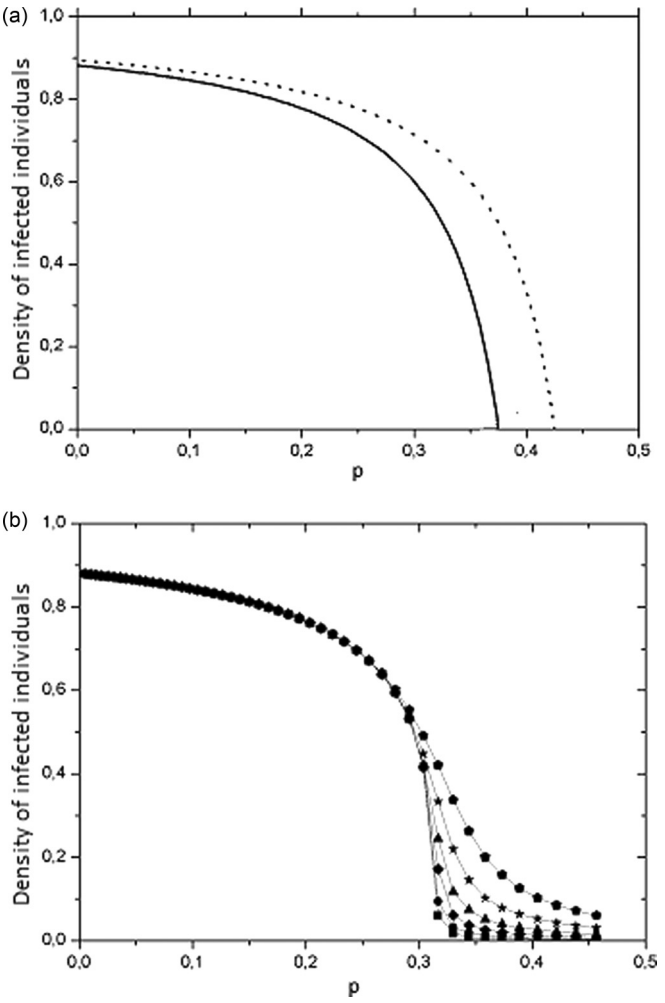

FIG. 7. In the SIRI model ($\alpha = 0$): the stationary density of infected individuals ρ versus p ($\rho \times p$) for a chain, with $\gamma = 0.05(\text{t.u.})^{-1}$, $x^* = 0$, and $\beta = (1-\gamma)/(1+\sigma)$, according to the condition (2); (a) for SMFA (solid line) and PMFA (dotted line); (b) for Monte Carlo simulations assuming $\zeta = 2$ and different values of L, $L = 20$, 40, 80, 160, 320, and 640, with the square symbol corresponding to the last one.

We construct the phase diagram for the SMFA making the change of variable

$$\begin{aligned} \alpha &= (1-\gamma)/2 - p, \\ \beta &= (1-\gamma)/2 + p, \\ \gamma &= \gamma, \end{aligned} \tag{14}$$

wherein the parameter $p = (\beta - \alpha)/2$ is set in the range $[-1/2, 1/2]$.

In this way, we can design the parameter space defined on the surface R^3 on a plane $p \times \gamma$. In Fig. 8, we observe no phase transition, i.e., the population remains in the *endemic* state. Thus, the density of infected individuals is not zero, and when $t \to \infty$, the number of susceptible individuals goes to zero.

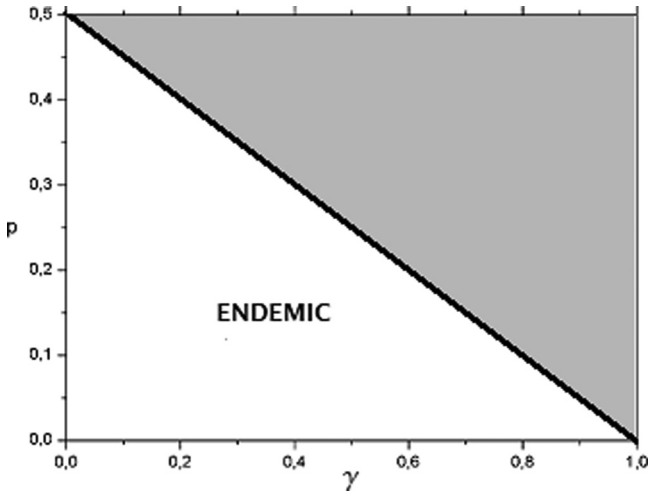

FIG. 8. Phase diagram of the SIRI model ($\alpha \neq 0$ and $\sigma = 0$) for the SMFA, wherein $p = (\beta - \alpha)/2$.

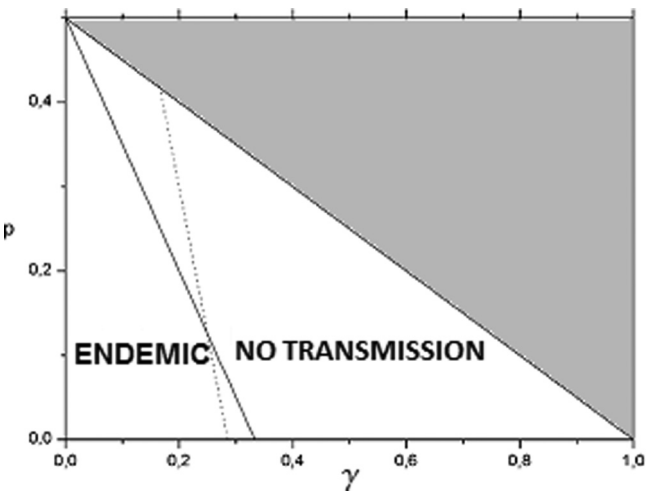

FIG. 9. Phase diagram of the SIRI model ($\alpha \neq 0$ and $\sigma = 0$) for PMFA, wherein $p = (\beta - \alpha)/2$; the lines $p_c = \frac{1}{2}[\gamma - 1 + \zeta(1 - 2\gamma)]$ for $\zeta = 2$ (solid line) and $\zeta = 4$ (dotted line).

B. PMFA ($\sigma = 0$)

Assuming $\sigma = 0$ in the system of Eq. (10), we obtain infinite number of fixed points $E = (x^*, y^*, u^*, v^*, w^*)$:

$$E = \left(x^*, D, 0, 0, \frac{D\gamma}{\alpha + \gamma}\right), \quad \forall\, x^* \neq 0,\ x^* \leqslant 1 \qquad (15)$$

wherein $D = \alpha(1 - x^*)/(\alpha + \gamma)$.

We also obtain, for the pair approximation, that the steady state does not depend on the coordination number ζ. This behavior is due to the fact that the transition $SI \to II$, that depends on the neighborhood, for long time, ceases to occur, remaining only the spontaneous transitions $I \to R$ and $R \to I$. Another difference in relation to the general case ($\sigma \neq 0$ and $\alpha \neq 0$) is that the trivial fixed point $E_0 = (1,0,0,0,0)$, which is the absorbing state of susceptible, is a possible solution.

The fixed point trivial E_0 will be stable if $\gamma > (\zeta - 2\beta)/(2\zeta)$. Making the change of variable (14) and using the condition (2), we have the critical threshold p in terms of γ:

$$p_c = \tfrac{1}{2}[\gamma - 1 + \zeta(1 - 2\gamma)]. \qquad (16)$$

For a chain ($\zeta = 2$) and a square lattice ($\zeta = 4$), the critical threshold is $p_c = (1 - 3\gamma)/2$ and $p_c = (3 - 7\gamma)/2$, respectively, and the stability occurs for values of $\gamma \leqslant \alpha$. Differently from SMFA, in pairs we observe a transition between the *endemic* and *no transmission* states, again assuming only positive values for rates.

We construct the phase diagram doing the same change of variable as in the SMFA. In Fig. 9, the phase diagram for pair approximation is shown; for $\zeta = 2$ there is a region of disease activity that is inactive for $\zeta = 4$ and vice versa.

V. DISCUSSION AND CONCLUDING REMARKS

We use the stochastic SIRI model to investigate the reinfection effect for directly transmitted diseases. Based on its master equation and the mean-field approximation analysis, we conclude that the pair approximation leads to a phase transition for the particular cases of exogenous reinfection (*endemic-epidemic*) or endogenous reactivation (*endemic–no transmission*). However, the phase transition is not observed if both effects are taken into account together; keep only the *endemic* state.

The phase diagram for $\alpha = 0$ is very interesting since it corresponds to a different phase diagram from the SIS to SIR model; the control parameter p measures the net effect of infection and reinfection. However, the *endemic* region is larger for $\zeta = 4$ than for $\zeta = 2$. Still for $\alpha = 0$, another very interesting phase diagram is observed for one-site mean-field approximation since there is a subregion of *epidemic* phase that coexists with *no transmission* phase (no transmission due to infection); its *endemic* region is larger than the *endemic* region for one-site mean-field approximation.

For the exogenous reinfection effect, we set up the threshold value of control parameter p, related the difference between the primary infection and reinfection, for both SMFA and PMFA, as well as for Monte Carlo simulations through the cumulant analysis. The results emphasize that PMFA is much better than SMFA to describe the dynamics of exogenous reinfection, leading to a smaller value of p, that means a larger value of reinfection parameter σ. Moreover, the arisen comparisons of the SIRI model with the limit cases of SIR and SIS models highlight its richness making evidence of the transition from the epidemic to endemic phases: the reinfection increases the peaks of outbreaks until the system reaches the endemic phase. Besides, it also important that, for a fixed non-null reinfection parameter, for any value of primary infection rate β, the intensity of the epidemics or endemics is stronger than for the limit cases, and its threshold values β_{th} are smaller than its values for the SIS and SIR models.

Concerning diseases such as tuberculosis that are typically endemic, the SIRI model is able to describe the reinfection effect. For both particular cases of exogenous reinfection and endogenous reactivation, the *endemic* phase is identified for lower values of both the recovered rate and the net result for reinfection in relation to infection ($0 < p < 1/2$).

The next step, still in the context of stochastic dynamics, consists in adding a latent compartment in the SIRI model called the exposed compartment, for which the individual is infected, but not infectious. In order to describe diseases with latent period in a more realist way, we intend to analyze the susceptible, exposed, infected, and removed or recovered (SEIR_E^I) model assuming $R \to E$ transition by exogenous reinfection and $R \to I$ transition by endogenous reactivation. Thus, the SEIR_E^I model should describe, in a more realistic way, diseases with latency period, such as tuberculosis.

Another consequent perspective of this work is to investigate situations for which SIRI model presents discontinuous phase transitions as we have observed in Erdós-Renyi networks when $\sigma > 1$ to describe the social contagions [17]. We conjecture that the increasing propagation of ideas may mimic the cooperative effect analogous to coinfections simulated by the SIR model with two different probabilities of infection [10,11] leading to abrupt transitions for Erdós-Renyi networks. Therefore, we intend to perform a systematic analysis of the SIRI model, for $\sigma < 1$ and $\sigma > 1$, on networks with different topologies.

Finally, that analysis may be extended for d-dimensional lattices with different values of d. As for the SIS model [28] and SIR model [30], whose upper dimension to recover the critical exponents of SMFA are, respectively, $d_{\mathrm{MF}} = 4$ and $d_{\mathrm{MF}} = 6$, we expect that there is an upper dimension to characterize the continuous phase transition of the SIRI model for $\alpha = 0$ and $\sigma < 1$.

ACKNOWLEDGMENTS

We acknowledge the stimulating discussions with T. Tomé, M. de Oliveira, D. Souza, S. Ferreira, R. Andrade, and J. Gomez-Gardenes on stochastic dynamics and SIRI model. This work was partially supported by the INCT-Citecs (Contract No. 57 386 / 2008-9) (MCT-CNPq, Brazil) and the Pronex- FAPESB (PNX 0006/2009 contract).

[1] J. D. Murray, *Mathematical Biology: An Introduction* (Springer, New York, 2002).
[2] F. Brauer and C. Castilho-Chaves, *Mathematical Models in Population Biology and Epidemiology* (Cambridge University Press, Cambridge, 2005).
[3] R. M. Anderson and R. M. May, *Infectious Diseases of Humans Dynamics and Control* (Oxford Science, London, 2008).
[4] M. J. Keeling and P. Rohani, *Modeling Infectious Diseases in Humans and Animals* (Princeton University Press, Princeton, NJ, 2008).
[5] J. C. Miller, Phys. Rev. E **87**, 060801 (2013).
[6] J. Sanz, C.-Y. Xia, S. Meloni, and Y. Moreno, Phys. Rev. X **4**, 041005 (2014).
[7] M. G. M. Gomes, A. O. Franco, M. C. Gomes, and G. F. Medley, Proc. R. Soc. London B **271**, 617 (2004).
[8] M. J. Keeling and K. T. D. Eames, J. R. Soc. Interface **2**, 295 (2005).
[9] N. Araújo, P. Grassberger, B. Kahng, and K. J. Schrenk, Europhys. J.: Spec. Top. **223**, 2307 (2014).
[10] W. Cai, L. Chen, F. Ghanbarnejad, and P. Grassberger, Nat. Phys. **11**, 936 (2015).
[11] P. Grassberger, L. Chen, F. Ghanbarnejad, and W. Cai, Phys. Rev. E **93**, 042316 (2016).
[12] A. T. C. Silva, V. R. V. Assis, S. T. R. Pinho, T. Tomé, and M. J. de Oliveira, Phys. A (Amsterdam) **468**, 131 (2017).
[13] M. G. M. Gomes, L. J. White, and G. F. Medley, J. Theor. Biol. **236**, 111 (2005).
[14] J. S. Lopes, P. Rodrigues, S. T. R. Pinho, R. F. S. Andrade, R. Duarte, and M. G. Gomes, BMC Infec. Dis. **14**, 340 (2014).
[15] N. S. Goel and N. Richter-Dyn, *Stochastic Models in Biology* (Academic, New York, 1974).
[16] N. T. J. Bailey, Biometrika **40**, 177 (1953).
[17] J. G. Gardeñes, A. S. Barros, S. T. R. Pinho, and R. F. S. Andrade, Europhys. Lett. **110**, 58006 (2015).
[18] J. Martins, A. Pinto, and N. Stollenwerk, Phys. Lett. A **371**, 379 (2007).
[19] J. Martins, A. Pinto, and N. Stollenwerk, J. Biol. Dynam. **3**, 479 (2009).
[20] F. M. Ruziska, T. Tomé, and M. J. de Oliveira, Phys. A (Amsterdam) **467**, 21 (2017).
[21] L. J. White, M. J. Cox, and G. F. Medley, J. Math. Appl. Med. Biol. **15**, 211 (1998).
[22] R. Águas, G. Gonçalves, and M. G. M. Gomes, Lancet Infect. Dis. **6**, 112 (2006).
[23] J. D. Cherry, New Engl. J. Med. **367**, 785 (2012).
[24] M. G. M. Gomes, L. J. White, and G. F. Medley, J. Theor. Biol. **228**, 539 (2004).
[25] T. Tomé and R. M. Ziff, Phys. Rev. E **82**, 051921 (2010).
[26] D. R. de Souza, T. Tomé, and R. M. Ziff, J. Stat. Mech. (2011) P03006.
[27] T. E. Harris, Ann. Probab. **2**, 969 (1974).
[28] J. Marro and R. Dickman, *Nonequilibrium Phase Transitions in Lattice Models* (Cambridge University Press, Cambridge, 1999).
[29] T. Tomé and M. J. de Oliveira, Phys. Rev. E **72**, 026130 (2005).
[30] T. Tomé and M. J. de Oliveira, *Stochastic Dynamics and Irreversibility* (Springer, Heidelberg, 2015).